

Metabolic, cardiac and renal effects of the slow hydrogen sulfide-releasing molecule GYY4137 during resuscitated septic shock in swine with pre-existing coronary artery disease

Benedikt L. Nußbaum^{1,2}, Josef Vogt², Ulrich Wachter², Oscar McCook², Martin Wepler^{1,2}, José Matallo², Enrico Calzia², Michael Gröger², Michael Georgieff¹, Mark E. Wood³, Matthew Whiteman⁴, Peter Radermacher², Sebastian Hafner^{1,2}

¹Klinik für Anästhesiologie, Universitätsklinik Ulm, Germany; ²Institut für Anästhesiologische Pathophysiologie und Verfahrensentwicklung, Universitätsklinik Ulm, Germany; ³Department of Biosciences, College of Life and Environmental Science, University of Exeter, UK; ⁴University of Exeter Medical School, St. Luke's Campus, Exeter, UK

Corresponding author: Benedikt Nußbaum, M.D., Institut für Anästhesiologische Pathophysiologie und Verfahrensentwicklung, Universitätsklinik Ulm, Helmholtzstraße 8/1, 89081 Ulm, Germany, telephone number: 0049 731 500 60244, fax number: 0049 731 500 60162, e-mail address: benedikt.nussbaum@uni-ulm.de

Conflicts of interest and sources of funding: The authors declare no conflicts of interest. The study was supported by a grant from the Perspektivförderung Innovationsfond Medizin Land Baden-Württemberg.

Running Head: GYY4137 in septic shock in atherosclerotic swine

Abstract

Decreased levels of endogenous hydrogen sulfide (H₂S) contribute to atherosclerosis, whereas equivocal data are available on H₂S effects during sepsis. Moreover, H₂S improved glucose utilization in anaesthetized, ventilated, hypothermic mice, but normothermia and/or sepsis blunted this effect. The metabolic effects of H₂S in large animals are controversial. Therefore, we investigated the effects of the H₂S donor GYY4137 during resuscitated, fecal peritonitis-induced septic shock in swine with genetically and diet-induced coronary artery disease (CAD). 12 and 18 hours after peritonitis induction, pigs received either GYY4137 (10 mg·kg⁻¹, n=9) or vehicle (n=8). Before, at 12 and 24 hours of sepsis, we assessed left ventricular (pressure-conductance catheters) and renal (creatinine clearance, blood NGAL levels) function. Endogenous glucose production and glucose oxidation were derived from the plasma glucose isotope and the expiratory ¹³CO₂/¹²CO₂ enrichment during continuous i.v. 1,2,3,4,5,6-¹³C₆-glucose infusion. GYY4137 significantly increased aerobic glucose oxidation, which coincided with higher requirements of exogenous glucose to maintain normoglycemia, as well as significantly lower arterial pH and decreased base excess. Apart from significantly lower cardiac eNOS expression and higher troponin levels, GYY4137 did not significantly influence cardiac and kidney function or the systemic inflammatory response. During resuscitated septic shock in swine with CAD, GYY4137 shifted metabolism to preferential carbohydrate utilization. Increased troponin levels are possibly due to reduced local NO availability. Cautious dosing, the timing of GYY4137 administration and interspecies differences most likely account for the absence of any previously described anti-inflammatory or organ-protective effects of GYY4137 in this model.

Keywords: gluconeogenesis, glucose oxidation, eNOS, iNOS, CSE, HO-1, 3-nitrotyrosine, troponin

Introduction

Recent rodent studies have demonstrated that impaired endogenous hydrogen sulfide (H_2S) production is implicated in the pathogenesis of atherosclerosis (1). However, equivocal results are available on H_2S levels in patients with coronary artery disease (CAD): both reduced (2) and increased H_2S plasma levels (3) were described.

H_2S was also reported to affect glucose metabolism: Increased gluconeogenesis in hepatocytes following stimulation with sodium hydrosulfide (NaHS) was demonstrated in vitro (4), whereas CSE (cystathionine γ -lyase) knockout mice revealed reduced gluconeogenesis (5). Previously, we demonstrated that inhaled H_2S increased glucose oxidation in anaesthetized and mechanically ventilated mice during hypothermia, whereas both normothermia and/or sepsis blunted this effect (6).

The vast majority of data on H_2S with respect to glucose metabolism and cardiovascular properties originate from healthy small animal models, where H_2S is able to induce profound hypometabolism (7). The metabolic properties of H_2S in large animal models are controversial, inasmuch as both absence of metabolic effects (8-10) as well as reduced energy expenditure (11) were reported. Thus, the relevance and translatability of H_2S effects reported in small animals has been questioned for large animal models or humans (6, 12).

Due to the plethora of cardiovascular and metabolic effects of H_2S , H_2S -donating or inhibiting compounds are considered as promising future therapeutic options. While inhalation of gaseous H_2S is associated with pulmonary toxicity and airway irritation, intravenous application of sulfide salts face extremely narrow timing and dosing margins (13). GYY4137 (morpholin-4-ium-4-methoxyphenyl(morpholino) phosphinodithioate) is a slow-releasing H_2S donor with improved pharmacokinetics and a more constant release of H_2S compared to the instantaneous liberation by conventional sulfide salts (14), thus more closely mimicking endogenous H_2S release. GYY4137 demonstrated anti-inflammatory effects upon lipopolysaccharide (LPS) stimulation both in vitro and in rodents in vivo (15, 16). Up to now, no data are available about GYY4137 in large animals. Given the importance of H_2S in cardiovascular pathophysiology and its ambiguous metabolic role in large animals, we investigated the effects of GYY4137 in a clinically relevant porcine model of resuscitated septic shock with pre-existing atherosclerosis-induced CAD.

Materials and Methods

Animals

The study was approved by the University of Ulm Animal Care Committee and the Federal Authorities for Animal Research (animal experiment number 1098, date of approval by the Regierungspräsidium Tübingen: 22.05.2012). The experiments were performed in adherence with the National Institute of Health Guidelines on the Use of Laboratory Animals and the European Union "Directive 2010/63/EU on the protection of animals used for scientific

purposes". Eighteen castrated male familial hypercholesterolemia Bretoncelles Meishan (FBM) pigs with a median age of 19 months (interquartilerange (IQR): 18 to 20 months) and a median weight of 59 kg (IQR: 55 to 62 kg) were recruited for the study. One pig from the vehicle group was excluded from the study, as it had not developed diffuse peritonitis upon necropsy. Moreover, the pig did not require norepinephrine support, and thus, by definition, did not develop septic shock. Subsequent data refer to the 17 pigs included in the data analysis. The FBM pig strain is a cross-breed of Rapacz pigs with smaller strains (Chinese Meishan and Bretoncelles), characterized by a homozygous R84C low-density lipoprotein (LDL) receptor mutation, and develops marked atherosclerosis and consecutive CAD upon atherogenic diet (17). Animals received the diet (1 kg daily, 1.5 % cholesterol, 20 % bacon fat) for at least 9 months prior to the experiments. The phenotype has been characterized previously. Briefly, FBM pigs on atherogenic diet exhibit significantly higher cholesterol levels compared to healthy German landrace swine of the same age. Plasma levels of isoprostanes are significantly increased, while plasma nitrite/nitrate levels are significantly lower than in healthy control strains. FBM pigs are also characterized by a significantly lower creatinine clearance compared to healthy German landrace swine (18).

Anesthesia

Before the experiments, pigs were fasted for 12 hours with free access to water. Intramuscular premedication consisted of 5 mg kg⁻¹ azaperone. After establishment of an intravenous access via ear vein, anesthesia was induced with propofol (1-2 mg kg⁻¹) and ketamine (1-2 mg kg⁻¹). The pigs were endotracheally intubated and mechanically ventilated (tidal volume 8 ml kg⁻¹, respiratory rate 8 – 12 min⁻¹ adapted to achieve an arterial pCO₂ of 35 – 40 mmHg, inspiratory/expiratory (I/E) ratio 1:1.5, fraction of inspiratory oxygen (FiO₂) 30%, positive end expiratory pressure (PEEP) 10 cm H₂O to prevent formation of atelectasis, peak airway pressure ≤ 40 mmHg). Anesthesia was maintained with continuous intravenous infusion of pentobarbitone (8 – 12 mg kg⁻¹ h⁻¹). Buprenorphine was used for analgesia (30 µg kg⁻¹ initially, further 10 µg kg⁻¹ every 8 hours as well as prior to surgery and induction of fecal peritonitis). Pancuronium (0.15 mg kg⁻¹ h⁻¹) ensured muscle relaxation. Balanced electrolyte solutions (20 ml kg⁻¹ h⁻¹, Jonosteril 1/1, Fresenius, Bad Homburg, Germany) were infused for fluid homeostasis. During surgery, hydroxyethyl starch 6% 130/0.42 (Vitafusal, Serumwerk, Bernburg, Germany) was used to maintain filling pressures. External heating allowed to control and maintain body core temperature at 37.5 – 38.5° Celsius.

Surgical procedures

The right internal jugular vein was exposed and a 9F central venous catheter sheath was inserted. The central venous catheter was subsequently used for infusion therapy and application of intravenous drugs. A balloon-tipped thermodilution pulmonary artery catheter was inserted via the sheath and used for the measurement of central venous pressure (CVP), mean pulmonary artery pressure (MPAP), pulmonary artery occlusion pressure (PAOP) and cardiac output (CO). One femoral artery and the left carotid artery were exposed for placement of a PiCCO[®] catheter for continuous cardiac output measurement and an 8F arterial catheter sheath, respectively. A pressure-conductance catheter (CD Leycom, Hengelo,

The Netherlands) was inserted via the latter, and advanced into the left ventricle (LV) under control of the pressure curve. In order to determine kidney blood flow, a laparotomy was performed, and an ultrasonic flow probe was placed around the right kidney artery. Following exposure of a femoral vein, a 4F catheter was advanced into the inferior vena cava and guided into the right renal vein under manual and visual control. An indwelling catheter in the urinary bladder allowed urine collection. Two tubes were placed through the abdominal wall into the peritoneal cavity for subsequent induction of peritonitis.

Experimental protocol

After four hours of surgery, pigs were allowed to recover for eight hours before baseline data were collected. Subsequently, fecal peritonitis was induced. For this purpose, 1 g kg⁻¹ autologous feces was collected during premedication, dissolved in 500 ml 0.9% saline and incubated at 38° Celsius for 12 hours. 3 ml kg⁻¹ of the supernatant were injected into the peritoneal cavity via the abdominal tubes. 12 and 18 hours after induction of peritonitis, animals received bolus injections of 10 mg kg⁻¹ GYY4137 (n=9) or vehicle (saline, n=8). GYY4137 was synthesized in-house as previously described (14). Based on the time course of fecal peritonitis in previous sepsis studies of our group (19), where norepinephrine requirements to maintain baseline MAP indicated the onset of sepsis-induced hemodynamic alterations after 6 to 9 hours after peritonitis induction, the administration of GYY4137 was carried out as a “therapeutic approach” after development of sepsis. Balanced electrolyte solutions (20 ml kg⁻¹ h⁻¹) were continuously infused, and reduced to 10 ml kg⁻¹ h⁻¹ if PAOP > 18 mmHg. If MAP remained below baseline values despite volume resuscitation, norepinephrine was used to stabilize MAP at pre-peritonitis values. However, infusion rates of norepinephrine were not further increased, if the heart rate was higher than 160 min⁻¹ in order to avoid tachycardia-induced myocardial ischemia. Respirator settings were modified (I/E ratio 1:1, PEEP 12 or 15 cm H₂O) during the experiments when the ratio of the arterial oxygen partial pressure (p_aO₂) to FiO₂ dropped below 300 or 200 mmHg, respectively. FiO₂ was stepwise adjusted to maintain ap_aO₂ of 70-90 mmHg. At the end of the experiment, pigs were euthanized under deep anesthesia via injection of potassium chloride.

Measurements and calculations

Immediately before, 12 and 24 hours after induction of fecal peritonitis, data sets were collected. Measurements included haemodynamics (MAP, MPAP, PAOP, CVP, heart rate, CO), gas exchange (calorimetric CO₂ production, arterial and mixed venous blood gases (p_aO₂, p_aCO₂), pH, base excess, glucose, lactate, β-hydroxybutyrate and the plasma levels of troponin, interleukin (IL)-6, IL-1β, tumor necrosis factor alpha (TNFα), nitrite plus nitrate (NO₂⁻ + NO₃⁻) and 8-isoprostane. The pressure-conductance catheter allowed assessment of systolic and diastolic LV function. Renal function was assessed by determination of the following parameters: urine output, right kidney artery flow, renal venous blood gases, plasma creatinine and neutrophil gelatinase-associated lipocalin (NGAL) concentrations and creatinine clearance.

Using a steady state approach, endogenous glucose production was calculated after determination of plasma glucose isotope enrichment by combined gas chromatography/mass spectrometry (GC/MS) and correction for exogenous glucose administration during continuous intravenous infusion of stable, non-radioactively labeled 1,2,3,4,5,6-¹³C₆-glucose (tracer). Pigs received an initial priming dose of 400 mg of tracer over three hours. Subsequently, the tracer was continuously infused at a rate of approximately 0.025 mg kg⁻¹ min⁻¹ until the end of the experiment. Additional analysis of the enrichment of ¹³CO₂/¹²CO₂ isotope in the expiratory gas using non-dispersive infrared spectrometry together with the calorimetric determination of total CO₂ production allowed the calculation of the percentage of oxidized tracer and total aerobic glucose oxidation rate(19).

Free blood sulfide concentrations were determined by combined GC/MS(20).

Kidney and heart specimen were immediately collected post-mortem and analyzed for protein expression of heme oxygenase-1 (HO-1), B-cell lymphoma-extra large (Bcl-xL), inhibitor of nuclear factor kappa B (IκBα), the constitutive, endothelial and the inducible isoforms of nitric oxide synthase (eNOS, iNOS) by western blotting. Activation of the nuclear transcription factor kappa B (NF-κB) was assessed by electrophoretic mobility shift assay (EMSA). Actin and vinculin served as loading controls. For comparison between individual gels, the intensity of each band was related to that of the mean of two native animals, which had not undergone surgical instrumentation and fecal peritonitis. Western blots were run at least in triplicates. The mean value of the individual gels for each animal was used for quantitative analysis, and data are reported as fold increase over the mean of the two native animals. Supplemental figure 1, <http://links.lww.com/SHK/A550>, shows original western blots and EMSA for kidney (A) and heart (B) of all individual animals.

Additional heart and kidney specimens were taken for immunohistochemistry analysis of 3-nitrotyrosine formation, expression of the endogenous H₂S-producing enzyme CSE and extravascular albumin. Therefore, specimen were fixed in formalin, embedded in paraffin, dewaxed in xylene, and rehydrated with a graded series of ethanol. After incubation in citrate buffer and boiling for heat-induced antigen retrieval, samples were blocked with goat sera and subsequently incubated with primary anti-nitrotyrosine (polyclonal rabbit; Merck Millipore, Darmstadt, Germany), anti-CSE (monoclonal mouse; Abnova, Taipei City, Taiwan) or anti-albumin antibodies (polyclonal rabbit; Abcam, Cambridge, United Kingdom). Primary antibody detection was performed by using the Dako REAL Detection system/RED(Dako Deutschland GmbH, Hamburg, Germany), followed by counterstaining with haematoxylin. Slides were visualized using a Zeiss Axio Imager A1 microscope with a x10 objective. Quantification for intensity was performed using the AxioVision 4.8 software (Zeiss, Jena, Germany). Results are presented as mean densitometric sum red(19).

Mitochondrial respiratory activity was analyzed via “high-resolution respirometry” using the Oroboros Oxygraph-2K (Oroboros Instruments, Innsbruck, Austria) in homogenized cardiac, renal and hepatic tissue specimens collected at the end of the experiment. After supplementation of substrates for complexes I and II and ADP, maximal oxidative phosphorylation (in the coupled state, OxPhos) was assessed. Maximal respiratory capacity

of the electron transfer system (ETS) in the uncoupled state was measured after addition of 4-(trifluoromethoxy) phenylhydrazine (FCCP). Additionally, LEAK respiration compensating for proton leakage or slipping was reported as percentage of ETS capacity(21).

Statistical analysis

All data are expressed as median (IQR) unless otherwise stated. The effects of GYY4137 were analyzed using repeated measures (RM) two-way ANOVAs. P values for effects of time and treatment are reported in the data tables. Subsequent post-hoc testing within the ANOVAs was corrected for multiple comparisons (Sidak method). As GYY4137 was administered 12 and 18 hours after the induction of fecal peritonitis, i.e., after the 12 hour time point, the ANOVAs were performed with the 12 hour time point as baseline (before administration of GYY4137) and the 24 hour time point (after administration of GYY4137). Inter-group differences of data with only one data set (e.g. histology at the end of the experiments etc.) were analyzed by the Mann-Whitney rank sum test. A p value of less than 0.05 was considered statistically significant. GraphPad Prism 7 software was used for statistical evaluation and graphical display. A statistical sample size calculation based on creatinine levels and norepinephrine requirements of a previous study (13) and a power of 80% yielded a minimum of n=8 animals per group. In order to compensate for non-normal distribution of parameters, n=9 animals were recruited per group. The results should be interpreted carefully in an explorative manner due to the small sample size and the multitude of analyzed variables.

Results

Table 1 shows that sepsis and resuscitation caused a normotensive, hyperdynamic circulation in both groups. Comparable high doses of norepinephrine (0.90 (0.82; 1.18) vs 0.85 (0.54; 1.30) $\mu\text{g} \cdot \text{kg}^{-1} \cdot \text{min}^{-1}$, p=0.96) were required to maintain MAP in the GYY4137 and the control group, respectively. Further hemodynamic parameters (CVP, MPAP, PAOP) were also similar between groups. P_aO_2 and the p_aO_2 to FiO_2 ratio significantly declined after 24 hours, again without any intergroup differences.

Metabolic data before induction of fecal peritonitis comprising temperature, pH, base excess, plasma lactate, β -hydroxybutyrate (table 1), blood glucose, endogenous glucose production, glucose oxidation and CO_2 production from glucose oxidation (figure 1) were similar in the two groups. Endogenous glucose release slightly increased after 12 hours of peritonitis induction, and thereafter even decreased again in both groups (figure 1). After administration of GYY4137, pigs showed significantly higher tracer oxidation (p=0.041) and total glucose oxidation rate (p=0.020) at 24 hours compared to control animals, resulting in significantly higher requirement of exogenous glucose administration to maintain normoglycemia (p=0.018) (figure 1). While total CO_2 production remained constant in both groups between 12 and 24 hours after induction of fecal peritonitis (table 1), the fraction of CO_2 production from

glucose oxidation was significantly higher at 24 hours in the GYY4137-treated animals ($p=0.031$, figure 1).

Both arterial pH and base excess decreased after infusion of GYY4137 ($p<0.001$ and $p=0.051$, respectively). PH was significantly lower compared to vehicle at 24 hours ($p<0.001$), whereas lactate levels were comparable (table 1). Plasma sulfide levels did not significantly differ in the two groups either (table 2).

Table 3 demonstrates that blood biomarkers of inflammation and oxidative stress as well as nitrite/nitrate plasma levels did not significantly differ after 24 hours. However, blood isoprostanes were higher in the GYY4137 group 12 hours after induction of peritonitis, i.e. prior to the first injection of GYY4137.

Parameters of left ventricular function did not reveal substantial intergroup differences. However, troponin levels significantly increased in the GYY4137-treated pigs compared to before treatment ($p=0.01$) and were higher than in the control group at 24 hours ($p=0.059$, table 4). While cardiac Bcl-xL and HO-1 showed a non-significant trend towards reduced expression (both $p=0.07$), cardiac eNOS expression was significantly lower upon GYY4137 treatment ($p=0.001$, figure 2).

Apart from lower renal venous base excess ($p=0.001$) in the GYY4137 group at 24 hours, analysis of kidney function (table 5) and quantitative analysis of western blots for renal Bcl-xL, HO-1, I κ B α and iNOS expression as well as EMSA for NF- κ B activation (figure 3) did not show any further significant intergroup differences. Immunohistochemistry for renal and cardiac CSE expression, nitrotyrosine formation and extravascular albumin (figure 4), as well as mitochondrial respiratory capacity (Oxphos, ETS, LEAK/ETS) of cardiac, renal or hepatic tissue specimens (supplemental table 1, <http://links.lww.com/SHK/A551>) did not show any significant intergroup differences, either.

Discussion

Metabolic effects

In the present study, we investigated the effects of the slow-releasing hydrogen sulfide donor GYY4137 in a porcine model of resuscitated septic shock with pre-existing CAD. The main findings were significantly increased glucose oxidation (figure 1) and reduced arterial pH as well as base excess (table 1) in the GYY4137-treated pigs. As total CO₂ production did not increase, the higher glucose oxidation in the GYY4137 group supports the notion that GYY4137 treatment resulted in preferential carbohydrate utilization. Consistently, inhaled hydrogen sulfide also increased aerobic glucose oxidation in anesthetized and mechanically ventilated, hypothermic mice (6). Interestingly, in that study, normothermia and/or sepsis blunted the shift in substrate utilization. As both the metabolic rates and the metabolic response to stress substantially vary between small and large animals, interspecies differences might be responsible for the heterogeneous effects. Small rodents are able to rapidly reduce

their oxygen consumption and typically drop their core temperature in response to stress by reducing non-shivering thermogenesis without affecting ATP generation (6, 12), and H₂S-induced hypometabolism is well described (7, 22). In contrast, the decrease of the metabolic rate upon H₂S treatment remains a matter of debate in large animals or humans. In line with previous studies in pigs (9) or sheep (8, 10), H₂S-induced hypometabolism was absent in our study. Of note, while data from large animals were collected under anesthesia, the metabolic effects of H₂S in small mammals were predominantly reported in awake, spontaneously breathing mice (7) or rats (22). General anesthesia seems at least to attenuate hypometabolic effects of H₂S in mice (6).

Several studies demonstrated effects of H₂S on glucose metabolism. Stimulation of hepatocytes with NaHS impaired glucose utilization and increased gluconeogenesis *in vitro* (4), whereas genetic knockout of CSE decreased gluconeogenesis in mice (5). Incultured cardiomyocytes, NaHS, supported glucose uptake and metabolism in (23). Thus, H₂S might function as a provider of increased carbohydrate substrate availability by increasing hepatic glucose synthesis and by facilitating glucose utilization by other organs. Moreover, GYY4137 has been shown to inhibit lipolysis *in vivo* in mice receiving a high fat diet (24), further supporting a H₂S-induced shift in substrate utilization. Any shift towards carbohydrate oxidation entails an improved yield of the oxidative phosphorylation, as the net ATP production per mole of consumed oxygen is higher for carbohydrate than lipid oxidation (25).

Besides the influence of GYY4137 on glucose oxidation, pH was significantly lower at 24 hours of sepsis, and base excess decreased in the GYY4137 group. In contrast, plasma lactate levels were comparable (table 1). Hence, analyzing the strong ion difference (SID), the lactate levels could not account for the lower base excess. Accumulation of unmeasured acids such as free fatty acids due to the metabolic shift towards glucose utilization would be conceivable. However, β -hydroxybutyrate did not significantly differ among groups and even decreased at the end of the experiment in the GYY group (table 1). As both inhibitory and stimulatory effects of hydrogen sulfide on mitochondrial respiration have been described (26), we further excluded a possible toxic effect of GYY4137 on the mitochondrial respiratory capacity (supplemental table 1, <http://links.lww.com/SHK/A551>) as cause for the metabolic acidosis. Importantly, the mitochondrial results need to be interpreted very carefully: On the one hand, sample treatment and *ex-vivo* conditions might have blunted potential *in vivo* effects. On the other hand, as GYY4137 is not specifically targeted to the mitochondria, the amount of H₂S reaching the mitochondria might have been too low to provoke substantial effects. The effects of GYY4137 on the acid-base state remain elusive so far and deserve future investigation.

Non-metabolic results

Troponin levels were higher in the GYY4137 group at 24 hours (table 4). However, a trend towards increased troponin was already present 12 hours after induction of fecal peritonitis, i.e. prior to the injection of GYY4137. At that time point, plasma levels of 8-isoprostane were also higher than in the control group (table 3, $p=0.049$). Moreover, cardiac HO-1 expression

was lower in the GYY4137-treated pigs (figure 2). Finally, despite overall comparable doses of norepinephrine, the GYY4137-treated animals showed a tendency to increased cumulative doses of norepinephrine within the first 12 hours after induction of (0.61 (0.56; 0.79) vs 0.36 (0.28; 0.81) $\mu\text{g}\cdot\text{kg}^{-1}\cdot\text{min}^{-1}$; $p=0.11$). Thus, both more pronounced oxidative stress and enhanced myocardial O_2 demand resulting from higher norepinephrine needs might explain the increased troponin levels independently of GYY4137. After administration of GYY4137, 8-isoprostane levels slightly decreased supporting a previously described antioxidant role of GYY4137 in the heart (27). However, in contrast to studies in rodents reporting both NO-dependent and NO-independent cardioprotective effects of GYY4137 (28, 29), myocardial eNOS expression was significantly lower in the GYY4137-treated animals (figure 2). Consequently, reduced local availability of NO might have further contributed to cardiac injury. Of note, troponin levels were also elevated in a dose-dependent manner in a porcine model of cardiac arrest and resuscitation during supplementation of Na_2S (30). Interspecies differences or the pre-existing cardiac comorbidity might account for the different results.

In contrast to conventional sulfide donors (gaseous application, sulfide salts), GYY4137 more consistently displayed anti-inflammatory features in previous studies, both in vitro and in vivo (15, 16). Moreover, GYY4137 reduced kidney and liver damage during endotoxic shock in vivo (15). These anti-inflammatory and organ-protective properties of GYY4137 could not be demonstrated in the present study. However, all previous data on organ-protective effects of GYY4137 originate from studies in small mammals. Furthermore, intensive care measures and, in particular, the high-dose vasopressor support may have blunted potential GYY4137-mediated effects, as norepinephrine is well-established to have pro-oxidant properties, especially in the heart (31), and existing murine studies do not comprise standard ICU and catecholamine therapy. The pre-existing atherosclerotic comorbidity might also be accountable for the discrepant results. Decreased endogenous H_2S production has been implicated in the development of atherosclerosis (1). Finally, the most important aspects to consider are timing and dosing of GYY4137. As no studies about GYY4137 in large animals have been reported so far, dosing of GYY4137 was selected according to previous rodent experiments (14). In the initial study characterizing the novel compound GYY4137, a low dose of $26.6\ \mu\text{mol}\cdot\text{kg}^{-1}$ already caused a fall in MAP of more than 5 mmHg in rodents (14). In the present study, two boli of $10\ \text{mg}\cdot\text{kg}^{-1}$ ($26.6\ \mu\text{mol}\cdot\text{kg}^{-1}$) GYY4137 were administered 12 and 18 hours after peritonitis induction, and higher doses were not used in order to avoid aggravation of sepsis-induced hypotension due to vasodilatory effects of H_2S . Hence, the dose of GYY4137 may have limited the findings with respect to anti-inflammatory and organ-protective properties, and higher doses might have yielded further results, especially as H_2S liberation from GYY4137 has been shown to be rather slowly and less efficient compared to novel compounds (32). In addition, timing represents a crucial aspect for the efficacy of GYY4137 and H_2S -based therapies (13): The anti-inflammatory and organ-protective properties of GYY4137 in endotoxic shock in rats could only be seen when GYY4137 was given shortly (1 or 2 hours) after LPS injection, whereas a pre-treatment design failed to induce significant anti-inflammatory effects (15). Due to temporal differences in the evolution of sepsis-induced alterations between the rodent model

of endotoxic shock and our porcine model of fecal peritonitis, GYY4137 was given 12 and 18 hours after induction of peritonitis in the present study, when sepsis had fully developed. Thus, the dose of GYY4137 and the clinically relevant post-treatment administration of GYY4137 might account for the absence of anti-inflammatory and organ-protective results in the present study.

Measurement of free blood sulfide levels did not reveal significant differences between the GYY4137 and the control group (table 2). However, application of exogenous H₂S is not necessarily reflected in increased free sulfide blood levels due to the high sulfide-binding capacity of blood (33). Spiking of blood samples *ex vivo* with sodium sulfide to reach a target concentration of 100 μM only increased sulfide blood levels to about 20 μM (20). Moreover, in a previous study from our group, infusion of sodium sulfide attenuated kidney injury and reduced the inflammatory response after aortic occlusion, although blood sulfide levels were hardly affected (34). Thus, measured free blood sulfide levels do not need to correlate with biological effects, either, as H₂S-mediated effects might be due to intracellular H₂S, which is not detected by blood measurements. As the present study is the first to evaluate the effects of GYY4137 in swine, we cannot be certain whether the effects were due to intra- or extracellular H₂S generated from GYY4137, and in our *in vivo* study it was not possible to determine intracellular H₂S production. However, given the numerous previously described intracellular effects of GYY4137-derived H₂S (32) and the rapid rate of exogenous H₂S removal in blood (e.g. scavenging by hemoglobin etc.) together with the unaffected, measured blood sulfide levels, it is most likely, that the observed effects were due to intracellular H₂S released from GYY4137 rather than extracellular H₂S.

Limitations

As GYY4137 is a slow-releasing H₂S donor, that releases H₂S via hydrolysis, we cannot exclude the possibility, that the experimental results are influenced by either the mother substance itself or the residual molecule after H₂S liberation (“decomposed” GYY4137) (35). However, as a similar metabolic shift towards preferential carbohydrate utilization has been reported with inhaled H₂S in mice (6), the present results are most likely attributable to the released H₂S. Furthermore, “decomposed” GYY4137 did not exert similar cellular effects *in vitro* and *in vivo* compared to the original compound (15, 35), suggesting that the present results are due to GYY4137-derived H₂S. However, as discussed above, the dosage of GYY4137 might have limited the findings with respect to previously described anti-inflammatory or organ-protective properties and future studies in large animals should take higher dosing into account. Moreover, the metabolic properties with regard to glucose oxidation already slightly (but non-significantly) differed between the GYY4137 and the control group at the 12 hour time point before the application of GYY4137. Because of the small number of animals, we cannot fully exclude the possibility, that the effects reported for GYY4137 at 24 hours were due to uneven group distribution. Future studies need to validate the reported effects of GYY4137 in larger cohorts.

Another potential limitation represents the pre-existing cardiovascular comorbidity of the FBM swine. As previously reported effects of GYY4137 were evaluated *in vitro* and in

healthy in vivo models, the pre-existing hypercholesterolemia and CAD in our model might have influenced the effects of GYY4137 compared to healthy pigs.

Conclusion

To the best of our knowledge, this is the first study to evaluate effects of the slow-releasing H₂S donor GYY4137 in large animals. During resuscitated septic shock in swine with pre-existing atherosclerosis-induced CAD, GYY4137 shifted metabolism to preferential carbohydrate utilization under controlled normothermia and reduced arterial pH. Previously reported anti-inflammatory and organ-protective properties of GYY4137 in rodents could not be demonstrated most likely due to different timing and dosing of GYY4137. Increased troponin levels might be due to reduced local availability of NO and deserve further investigation.

Acknowledgements

We thank Bettina Stahl, Andrea Seifritz, Anja Gröger, Rosemarie Mayer, Marina Fink, Tanja Schulz, Rosa M. Engelhardt and Ingrid Eble for their skillful technical assistance.

References

1. Mani S, Li H, Untereiner A, Wu L, Yang G, Austin RC, Dickhout JG, Lhoták Š, Meng QH, Wang R: Decreased endogenous production of hydrogen sulfide accelerates atherosclerosis. *Circulation* 127 (25): 2523–2534, 2013.
2. Jiang H-L, Wu H-C, Li Z-L, Geng B, Tang C-S: [Changes of the new gaseous transmitter H₂S in patients with coronary heart disease]. *Di Yi Jun Yi Da Xue Xue Bao* 25 (8): 951–954, 2005.
3. Peter EA, Shen X, Shah SH, Pardue S, Glawe JD, Zhang WW, Reddy P, Akkus NI, Varma J, Kevil CG: Plasma free H₂S levels are elevated in patients with cardiovascular disease. *J Am Heart Assoc* 2 (5): e000387–e000387, 2013.
4. Zhang L, Yang G, Untereiner A, Ju Y, Wu L, Wang R: Hydrogen sulfide impairs glucose utilization and increases gluconeogenesis in hepatocytes. *Endocrinology* 154 (1): 114–126, 2013.
5. Untereiner AA, Wang R, Ju Y, Wu L: Decreased Gluconeogenesis in the Absence of Cystathionine Gamma-Lyase and the Underlying Mechanisms. *Antioxid. Redox Signal.* 24 (3): 129–140, 2016.
6. Asfar P, Calzia E, Radermacher P: Is pharmacological, H₂S-induced “suspended animation” feasible in the ICU? *Crit Care* 18 (2): 215, 2014.
7. Blackstone E, Morrison M, Roth MB: H₂S induces a suspended animation-like state in mice. *Science* 308 (5721): 518, 2005.
8. Haouzi P, Notet V, Chenuel B, Chalon B, Sponne I, Ogier V, Bihain B: H₂S induced hypometabolism in mice is missing in sedated sheep. *Respir Physiol Neurobiol* 160 (1): 109–115, 2008.
9. Drabek T, Kochanek PM, Stezoski J, Wu X, Bayr H, Morhard RC, Stezoski SW, Tisherman SA: Intravenous Hydrogen Sulfide Does Not Induce Hypothermia or Improve Survival from Hemorrhagic Shock in Pigs. *Shock* 35 (1): 67–73, 2011.
10. Derwall M, Francis RCE, Kida K, Bougaki M, Crimi E, Adrie C, Zapol WM, Ichinose F: Administration of hydrogen sulfide via extracorporeal membrane lung ventilation in sheep with partial cardiopulmonary bypass perfusion: a proof of concept study on metabolic and vasomotor effects. *Crit Care* 15 (1): R51, 2011.
11. Simon F, Giudici R, Duy CN, Schelzig H, Öter S, Gröger M, Wachter U, Vogt J, Speit G, Szabó C, Radermacher P, Calzia E: Hemodynamic and metabolic effects of hydrogen sulfide during porcine ischemia/reperfusion injury. *Shock* 30 (4): 359–364, 2008.
12. Haouzi P: Murine models in critical care research. *Crit Care Med* 39 (10): 2290–2293, 2011.

13. Bracht H, Scheuerle A, Gröger M, Hauser B, Matallo J, McCook O, Seifritz A, Wachter U, Vogt JA, Asfar P, Matejovic M, Möller P, Calzia E, Szabó C, Stahl W, Hoppe K, Stahl B, Lampl L, Georgieff M, Wagner F, Radermacher P, Simon F: Effects of intravenous sulfide during resuscitated porcine hemorrhagic shock*. *Crit Care Med* 40 (7): 2157–2167, 2012.
14. Li L, Whiteman M, Guan YY, Neo KL, Cheng Y, Lee SW, Zhao Y, Baskar R, Tan C-H, Moore PK: Characterization of a novel, water-soluble hydrogen sulfide-releasing molecule (GYY4137): new insights into the biology of hydrogen sulfide. *Circulation* 117 (18): 2351–2360, 2008.
15. Li L, Salto-Tellez M, Tan C-H, Whiteman M, Moore PK: GYY4137, a novel hydrogen sulfide-releasing molecule, protects against endotoxic shock in the rat. *Free Radic Biol Med* 47 (1): 103–113, 2009.
16. Whiteman M, Li L, Rose P, Tan C-H, Parkinson DB, Moore PK: The effect of hydrogen sulfide donors on lipopolysaccharide-induced formation of inflammatory mediators in macrophages. *Antioxid. Redox Signal.* 12 (10): 1147–1154, 2010.
17. Thim T, Hagensen MK, Drouet L, Bal Dit Sollier C, Bonneau M, Granada JF, Nielsen LB, Paaske WP, Bøtker HE, Falk E: Familial hypercholesterolaemic downsized pig with human-like coronary atherosclerosis: a model for preclinical studies. *EuroIntervention* 6 (2): 261–268, 2010.
18. Nussbaum BL, McCook O, Hartmann C, Matallo J, Wepler M, Antonucci E, Kalbitz M, Huber-Lang M, Georgieff M, Calzia E, Radermacher P, Hafner S: Left ventricular function during porcine-resuscitated septic shock with pre-existing atherosclerosis. *Intensive Care Med Exp* 4 (1): 14, 2016.
19. Wepler M, Hafner S, Scheuerle A, Reize M, Gröger M, Wagner F, Simon F, Matallo J, Gottschalch F, Seifritz A, Stahl B, Matejovic M, Kapoor A, Möller P, Calzia E, Georgieff M, Wachter U, Vogt JA, Thiemermann C, Radermacher P, McCook O: Effects of the PPAR- β/δ agonist GW0742 during resuscitated porcine septic shock. *Intensive Care Med Exp* 1 (1): 28, 2013.
20. McCook O, Radermacher P, Volani C, Asfar P, Ignatius A, Kemmler J, Möller P, Szabó C, Whiteman M, Wood ME, Wang R, Georgieff M, Wachter U: H₂S during circulatory shock: some unresolved questions. *Nitric Oxide* 41 48–61, 2014.
21. Vogt JA, Wachter U, Wagner K, Calzia E, Gröger M, Weber S, Stahl B, Georgieff M, Asfar P, Fontaine E, Radermacher P, Leverve XM, Wagner F: Effects of glycemic control on glucose utilization and mitochondrial respiration during resuscitated murine septic shock. *Intensive Care Med Exp* 2 (1): 19, 2014.
22. Seitz DH, Fröba JS, Niesler U, Palmer A, Veltkamp HA, Braumüller ST, Wagner F, Wagner K, Bäder S, Wachter U, Calzia E, Radermacher P, Huber-Lang MS, Zhou S, Gebhard F, Knöferl MW: Inhaled hydrogen sulfide induces suspended animation, but

does not alter the inflammatory response after blunt chest trauma. *Shock* 37 (2): 197–204, 2012.

23. Liang M, Jin S, Wu D-D, Wang M-J, Zhu YC: Hydrogen sulfide improves glucose metabolism and prevents hypertrophy in cardiomyocytes. *Nitric Oxide* 46 114–122, 2015.
24. Geng B, Cai B, Liao F, Zheng Y, Zeng Q, Fan X, Gong Y, Yang J, Cui QH, Tang C, Xu GH: Increase or decrease hydrogen sulfide exert opposite lipolysis, but reduce global insulin resistance in high fatty diet induced obese mice. *PLoS ONE* 8 (9): e73892, 2013.
25. Leverve XM: Mitochondrial function and substrate availability. *Crit Care Med* 35 (9 Suppl): S454–60, 2007.
26. Szabó C, Ransy C, Módis K, Andriamihaja M, Murgheș B, Coletta C, Olah G, Yanagi K, Bouillaud F: Regulation of mitochondrial bioenergetic function by hydrogen sulfide. Part I. Biochemical and physiological mechanisms. *Br J Pharmacol* 171 (8): 2099–2122, 2014.
27. Meng G, Wang J, Xiao Y, Bai W, Xie L, Shan L, Moore PK, Ji Y: GYY4137 protects against myocardial ischemia and reperfusion injury by attenuating oxidative stress and apoptosis in rats. *J Biomed Res* 29 (3): 203–213, 2015.
28. Chatzianastasiou A, Bibli S-I, Andreadou I, Efentakis P, Kaludercic N, Wood ME, Whiteman M, Di Lisa F, Daiber A, Manolopoulos VG, Szabó C, Papapetropoulos A: Cardioprotection by H₂S donors: nitric oxide-dependent and -independent mechanisms. *J. Pharmacol. Exp. Ther.* 2016.
29. Karwi QG, Whiteman M, Wood ME, Torregrossa R, Baxter GF: Pharmacological postconditioning against myocardial infarction with a slow-releasing hydrogen sulfide donor, GYY4137. *Pharmacol. Res.* 2016.
30. Derwall M, Westerkamp M, Löwer C, Deike-Glindemann J, Schnorrenberger NK, Coburn M, Nolte KW, Gaisa N, Weis J, Siepmann K, Häusler M, Rossaint R, Fries M: Hydrogen sulfide does not increase resuscitability in a porcine model of prolonged cardiac arrest. *Shock* 34 (2): 190–195, 2010.
31. Neri M, Cerretani D, Fiaschi AI, Laghi PF, Pietro Euea Lazzarini, Maffione AB, Micheli L, Bruni G, Nencini C, Giorgi G, D'Errico S, Fiore C, Pomara C, Riezzo I, Turillazzi E, Fineschi V: Correlation between cardiac oxidative stress and myocardial pathology due to acute and chronic norepinephrine administration in rats. *J. Cell. Mol. Med.* 11 (1): 156–170, 2007.
32. Whiteman M, Perry A, Zhou Z, Bucci M, Papapetropoulos A, Cirino G, Wood ME: Phosphinodithioate and Phosphoramidodithioate Hydrogen Sulfide Donors. *Handb Exp Pharmacol.* Vol. 230. Springer, 2015, pp 337–363.

33. Whitfield NL, Kreimier EL, Verdial FC, Skovgaard N, Olson KR: Reappraisal of H₂S/sulfide concentration in vertebrate blood and its potential significance in ischemic preconditioning and vascular signaling. *Am. J. Physiol. Regul. Integr. Comp. Physiol.* 294 (6): R1930–7, 2008.
34. Simon F, Scheuerle A, Gröger M, Stahl B, Wachter U, Vogt J, Speit G, Hauser B, Möller P, Calzia E, Szabó C, Schelzig H, Georgieff M, Radermacher P, Wagner F: Effects of Intravenous Sulfide During Porcine Aortic Occlusion-Induced Kidney Ischemia/Reperfusion Injury. *Shock* 35 (2): 156–163, 2011.
35. Alexander BE, Coles SJ, Fox BC, Khan TF, Maliszewski J, Perry A, Pitak MB, Whiteman M, Wood ME: Investigating the generation of hydrogen sulfide from the phosphoramidodithioate slow-release donor GYY4137. *Med. Chem. Commun.* 6 (9): 1649–1655, 2015.

ACCEPTED

Figure legends

Figure 1: Glucose metabolism analyzed by combined gas chromatography and mass spectrometry (GC/MS). Boxplots display median, quartiles and range. GYY4137 was administered 12 and 18 hours after induction of fecal peritonitis, i.e., after the 12 hour time point. vehicle: n=8; GYY4137 n=8; n=7 for endogenous glucose production. * p<0.05 compared to vehicle.

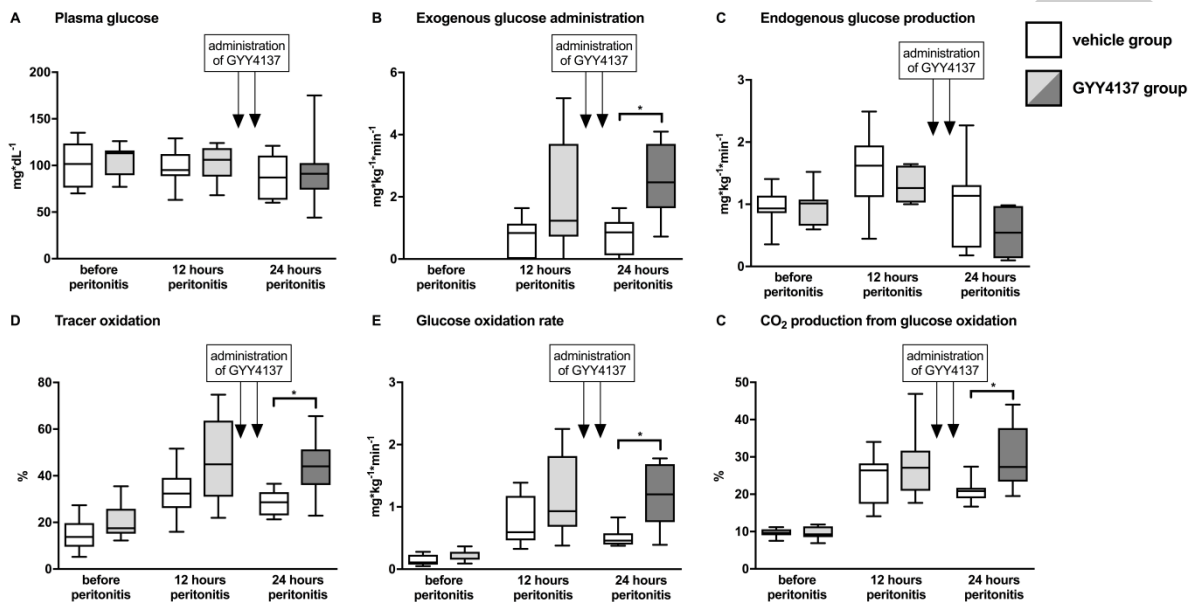


Figure 2: Quantitative analysis of western blots and electrophoretic mobility shift assay (EMSA) for Nf- κ B of heart specimens collected at the end of the experiment.

For comparison between individual gels, the intensity of each band was related to that of the mean of two native animals, which had not undergone surgical instrumentation and faecal peritonitis. The mean value of the individual gels for each animal was used for quantitative analysis, and data are reported as fold increase over the mean of the two native animals.

Boxplots display median, quartiles and range. vehicle: n=8 animals; GYY4137 n=7. eNOS: endothelial isoform of the nitric oxide synthase; iNOS: inducible isoforms of the nitric oxide synthase; HO-1: heme oxygenase-1; Bcl-xL: B-cell lymphoma-extra large; I κ B α : inhibitor of nuclear factor kappa B; NF- κ B: nuclear transcription factor kappa B.

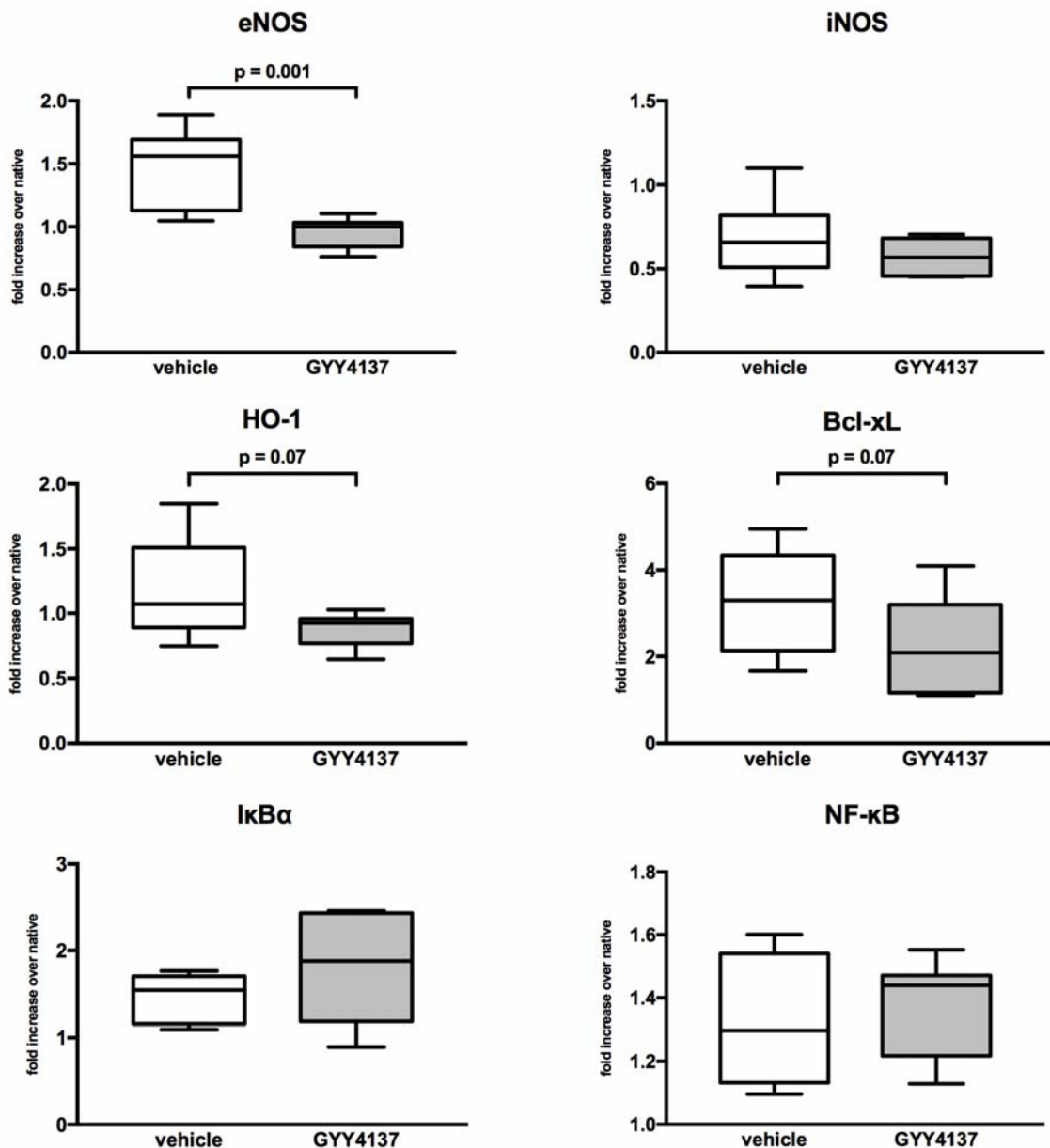


Figure 3: Quantitative analysis of western blots and electrophoretic mobility shift assay (EMSA) for Nf- κ B of kidney specimens collected at the end of the experiment.

For comparison between individual gels, the intensity of each band was related to that of the mean of two native animals, which had not undergone surgical instrumentation and fecal peritonitis. The mean value of the individual gels for each animal was used for quantitative analysis, and data are reported as fold increase over the mean of the two native animals.

Boxplots display median, quartiles and range. vehicle: n=8; GYY4137 n=9. Bcl-xL: B-cell lymphoma-extra large; HO-1: heme oxygenase-1; I κ B α : inhibitor of nuclear factor kappa B; iNOS: inducible isoforms of the nitric oxide synthase; NF- κ B: nuclear transcription factor kappa B.

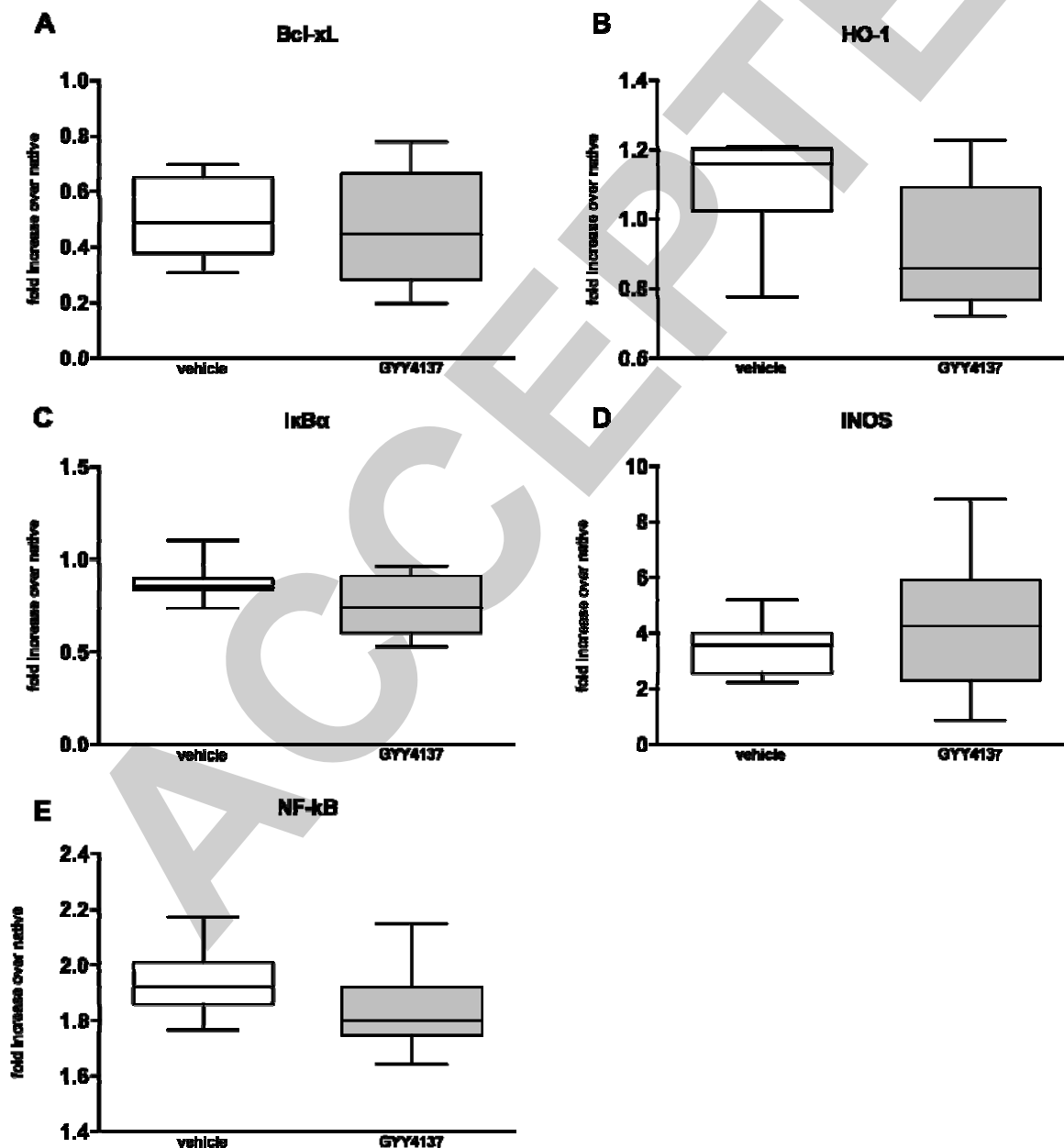
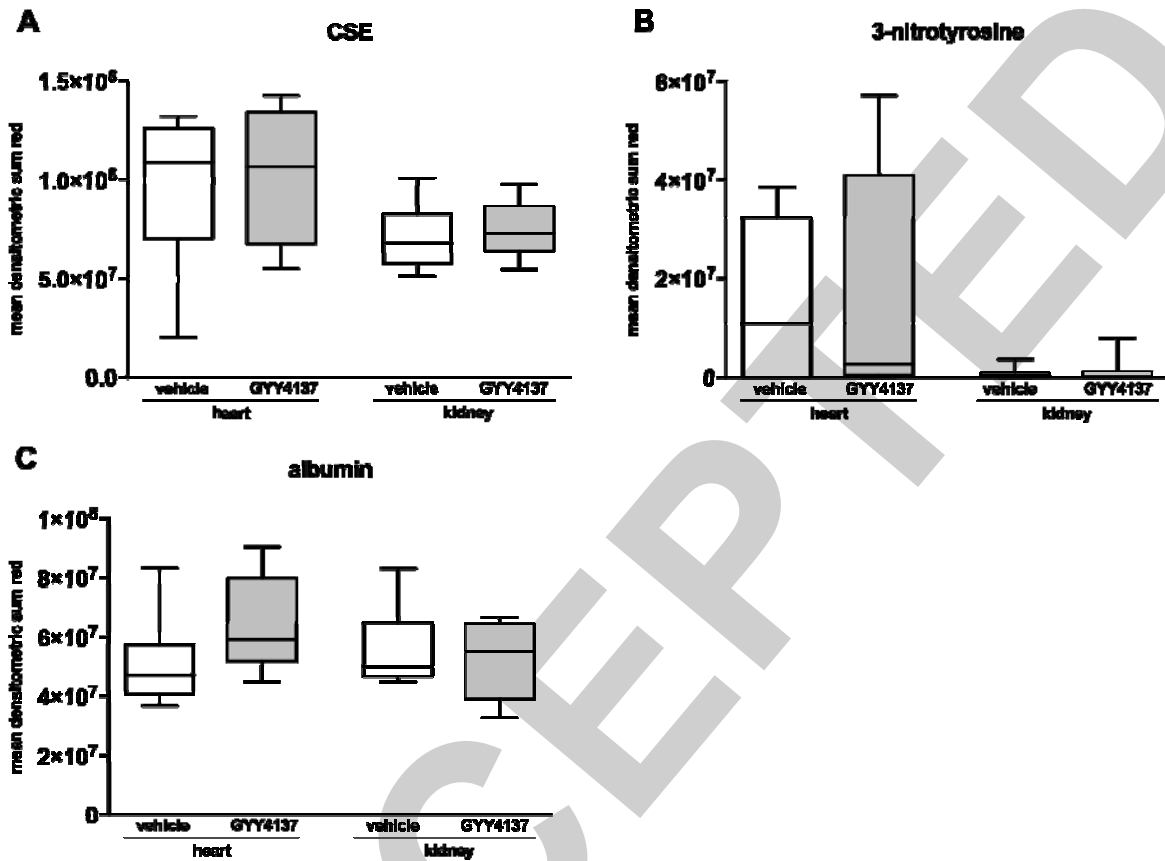


Figure 4: Immunohistochemistry of heart and kidney specimens collected at the end of the experiment.

Quantitative results of densitometric analysis. Boxplots display median, quartiles and range. vehicle: n=8 animals (except for heart (albumin): n=7); GYY4137 n=8 for heart, n=9 for kidney. CSE: cystathionine γ -lyase.



Supplemental Figure 1: Original western blots and electrophoretic mobility shift assays(EMSA) for Nf-κB of kidney (A) and heart (B) specimens collected at the end of the experiments.

For subsequent comparison between individual gels, the intensity of each band was related to that of the mean of two native animals, which had not undergone surgical instrumentation and fecal peritonitis. Actin and vinculin served as loading controls. Bcl-xL: B-cell lymphoma-extra large; HO-1: heme oxygenase-1; IκBα: inhibitor of nuclear factor kappa B; iNOS: inducible isoforms of the nitric oxide synthase; NF-κB: nuclear transcription factor kappa B; eNOS: endothelial isoform of the nitric oxide synthase.

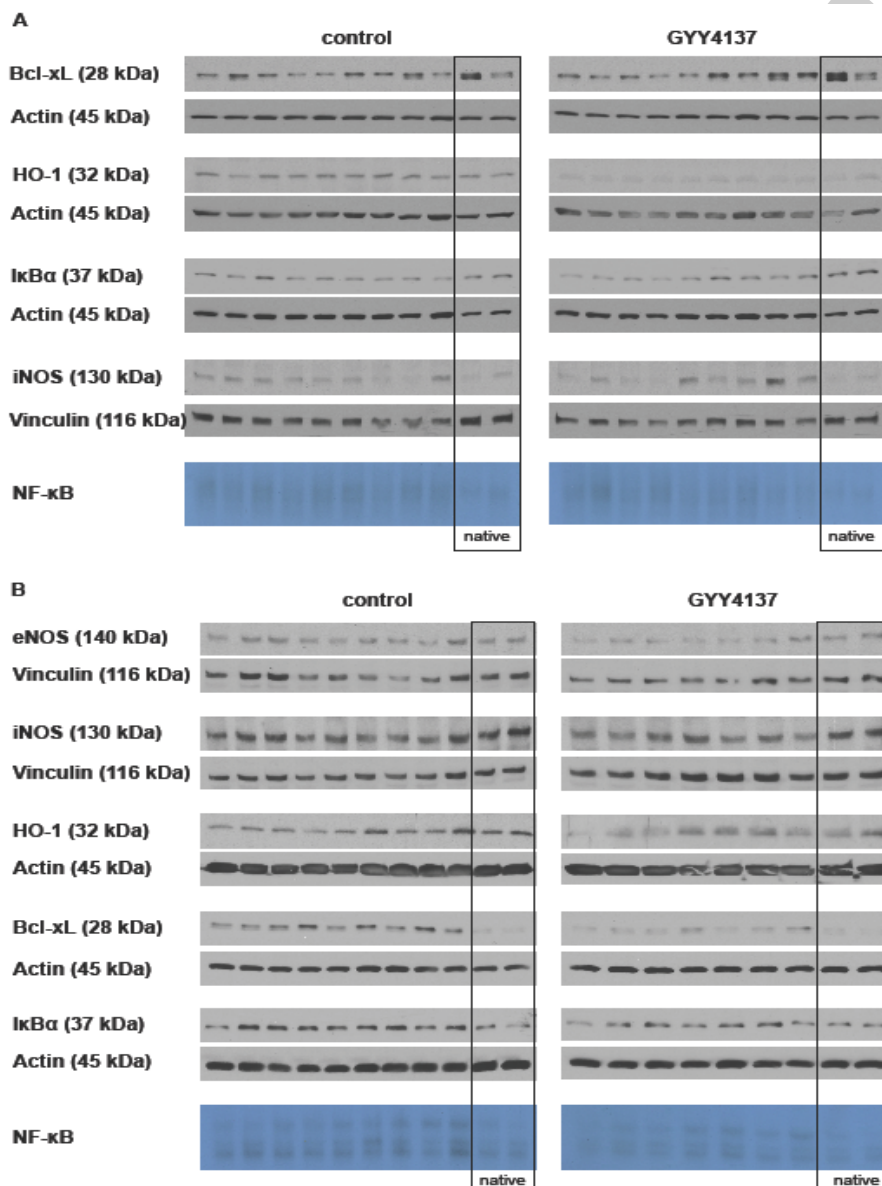


Table 1: Hemodynamics, gas exchange and acid base balance.

		before peritonitis	12 hours peritonitis	24 hours peritonitis	Repeated measures two-way ANOVA	
					p value for treatment	p value for time
Heart rate (min ⁻¹)	Vehicle GY4137	83 (73;96) 81 (65;99)	146 (107;157) 150 (137;157)	155 (151;173) [#] 164 (156;176) [#]	0.420	<0.001
Mean arterial pressure (mmHg)	Vehicle GY4137	97 (87;99) 96 (87;101)	93 (87;102) 92 (91;95)	87 (76;98) [#] 90 (82;97)	0.670	0.003
Mean pulmonary artery pressure (mmHg)	Vehicle GY4137	25 (23;29) 26 (25;28)	31 (27;39) 35 (30;37)	40 (32;43) [#] 40 (37;51) [#]	0.243	<0.001
Central venous pressure (mmHg)	Vehicle GY4137	13 (12;14) 14 (12;15)	13 (12;14) 14 (13;15)	17 (14;19) [#] 16 (15;19) [#]	0.498	<0.001
Pulmonary artery occlusion pressure (mmHg)	Vehicle GY4137	14 (12;17) 14 (13;17)	16 (13;16) 16 (14;17)	17 (14;19) 18 (16;20)	0.439	0.139
Cardiac output (L*min ⁻¹)	Vehicle GY4137	3.6 (2.4;4.9) 2.8 (2.6;3.6)	4.0 (3.6;4.7) 5.0 (4.3;5.5)	4.1 (2.5;4.4) 4.8 (3.8;5.3)	0.107	0.129
Arterial pO ₂ (mmHg)	Vehicle GY4137	140 (132;152) 138 (133;147)	126 (119;140) 130 (107;135)	97 (92;114) [#] 103 (83;107) [#]	0.272	<0.001
PaO ₂ /FIO ₂ ratio (mmHg)	Vehicle GY4137	467 (440;505) 460 (442;490)	420 (398;466) 433 (357;448)	324 (306;381) [#] 342 (278;355) [#]	0.202	<0.001
Arterial pCO ₂ (mmHg)	Vehicle GY4137	34 (32;37) 35 (34;37)	35 (33;36) 35 (33;37)	35 (33;37) 37 (35;40)	0.089	0.256
Body Temperature (°C)	Vehicle GY4137	37.2 (36.7;38.2) 37.0 (35.5;37.3)	38.0 (37.7;38.6) 38.1 (37.5;38.4)	37.9 (37.2;39.0) 38.1 (37.9;38.5)	0.744	0.253
Arterial pH	Vehicle GY4137	7.54 (7.50;7.57) 7.53 (7.47;7.53)	7.52 (7.50;7.52) 7.49 (7.46;7.54)	7.52 (7.50;7.52) 7.42 (7.41;7.46) ^{#,§}	0.009	<0.001
Arterial base excess (mmol*L ⁻¹)	Vehicle GY4137	6.2 (5.3;7.3) 6.3 (3.4;7.3)	5.5 (4.2;6.6) 4.0 (2.8;5.7)	4.3 (-4.6;5.5) 0.5 (-1.0;3.9)	0.571	0.006
Arterial lactate (mmol*L ⁻¹)	Vehicle GY4137	2.3 (1.8;2.6) 2.4 (1.9;3.3)	2.0 (1.4;2.5) 2.5 (1.8;2.9)	4.0 (2.3;5.8) [#] 4.3 (2.8;5.2) [#]	0.747	<0.001

beta-hydroxybutyrate ($\mu\text{mol}\cdot\text{L}^{-1}$)	Vehicle GY 4137	30.8 (20.2; 35.6) 38.2 (18.6; 45.7)	43.5 (22.8; 57.1) 48.8 (17.6; 82.3)	28.7 (16.2; 40.4) 12.7 (10.1; 27.1) [#]	0.546	0.007
CO₂ production (mL*kg⁻¹*min⁻¹)	Vehicle GY 4137	1.8 (1.4;2.2) 2.3 (2.1;2.7)	1.9 (1.7;2.6) 2.5 (2.1;3.3)	1.9 (1.6;2.5) 2.6 (2.1;3.5)	0.066	0.577

All data are expressed as median (25; 75 percentile). GYY4137 was administered 12 and 18 hours after induction of fecal peritonitis, i.e., after the 12 hour time point. Control n=8, GYY4137 n=9. #: p<0.05 vs 12 hours of peritonitis (before administration of GYY4137) within group.
§: p<0.05 vs vehicle.

Table 2: Free sulfide blood concentrations measured with combined gas chromatography/mass spectrometry.

		Before peritonitis	12 hours peritonitis	24 hours peritonitis	Repeated measures two-way ANOVA	
					p value for treatment	p value for time
Sulfide concentration [$\mu\text{mol}\cdot\text{L}^{-1}$]	Vehicle	1.4 (1.2;1.7)	1.8 (1.1;2.3)	2.4 (1.2;2.8)	0.717	0.083
	GY4137	1.2 (1.1;1.5)	1.2 (0.9;2.0)	1.5 (1.2;2.3)		

All data are expressed as median (25; 75 percentile). GY4137 was administered 12 and 18 hours after induction of fecal peritonitis, i.e., after the 12 hour time point. Control: n=8, GY4137 n=8 animals.

ACCEPTED

Table 3: Blood biomarkers of inflammation, oxidative and nitrosative stress.

		before peritonitis	12hours peritonitis	24hours peritonitis	Repeated measures two-way ANOVA	
					p value for treatment	p value for time
IL-1 β (pg*mL ⁻¹)	Vehicle	10 (10;10)	65 (47;85)	108 (85;333)	0.804	0.005
	GY Y 4137	10 (10;10)	47 (19;95)	154 (71;251)		
IL-6 (pg*mL ⁻¹)	Vehicle	97 (88;113)	952 (505;1704)	2166 (768;10820) [#]	0.372	0.006
	GY Y 4137	102 (82;164)	843 (363;1040)	2634 (1398;4547)		
TNF- α (pg*mL ⁻¹)	Vehicle	33 (23;37)	78 (63;109)	130 (89;154)	0.973	<0.001
	GY Y 4137	25 (20;34)	61 (49;74)	136 (122;184) [#]		
8-isoprostane (pg*mL ⁻¹)	Vehicle	53 (49;60)	72 (70; 101)	77 (71;142)	0.103	0.340
	GY Y 4137	59 (57;78)	128 (94; 175) [§]	102 (73;131)		
NO ₂ + NO ₃ (μ mol.L ⁻¹)	Vehicle	4.1 (3.4;5.0)	6.0 (5.1;7.7)	11.3 (8.7;16.5) [#]	0.494	<0.001
	GY Y 4137	4.6 (3.6;5.8)	5.7 (4.8;9.3)	14.7 (8.5; 17.0) [#]		

All data are expressed as median (25; 75 percentile). GYY4137 was administered 12 and 18 hours after induction of fecal peritonitis, i.e., after the 12 hour time point. Control: n=8, GYY4137 n=9 animals. #: p<0.05 vs 12 hours of peritonitis (before administration of GYY4137) within group. §: p<0.05 vs vehicle.

Table 4: Parameters of cardiac function and injury.

		before peritonitis	12 hours peritonitis	24 hours peritonitis	Repeated measures two-way ANOVA	
					p value for treatment	p value for time
Ejection fraction (%)	Vehicle GY4137	51 (48; 62) 40 (33; 70)	64 (45; 89) 46 (41; 62)	33 (23; 85) 33 (15; 54)	0.229	0.189
Stroke volume (mL)	Vehicle GY4137	51 (42; 58) 47 (39; 70)	49 (44; 57) 45 (41; 75)	44 (33; 54) 41 (37; 51)	0.954	0.166
Enddiastolic volume (mL)	Vehicle GY4137	91 (55; 104) 108 (61; 131)	62 (51; 69) 94 (56; 137)	73 (52; 128) 103 (68; 189)	0.030	0.066
Endsystolic pressure (mmHg)	Vehicle GY4137	111 (100; 114) 101 (94; 113)	103 (92; 109) 95 (86; 106)	107 (87; 111) 96 (91; 102)	0.490	0.808
Enddiastolic pressure (mmHg)	Vehicle GY4137	21 (20; 30) 20; 16;30)	20 (12; 34) 21 (15; 26)	25 (20; 38) 21 (8; 26)	0.198	0.265
dp/dt_{max} (mmHg*s⁻¹)	Vehicle GY4137	1972 (1890; 2286) 1988 (1605; 2175)	4000 (3460; 4383) 4606 (4122; 5726)	3251 (2469; 3941) 3803 (3103; 4383) [#]	0.125	0.001
dp/dt_{min} (mmHg*s⁻¹)	Vehicle GY4137	-2065 (-2576; -1913) -2106 (-2643; -1748)	-1931 (-2487; -1684) -2155 (-2756; -1583)	-2027 (-2448; -1512) -1876 (-2746; -1662)	0.734	0.586
Tau (ms)	Vehicle GY4137	36 (32; 45) 35 (32; 41)	31 (24; 48) 33 (20; 50)	26 (23; 36) 24 (20; 30)	0.583	0.485
Troponin (ng*ml⁻¹)	Vehicle GY4137	0.2 (0.0; 0.5) 0.1 (0.0; 0.3)	0.4 (0.1; 0.5) 0.9 (0.1; 1.8)	0.7 (0.4; 1.9) 1.6 (1.2; 2.9) [#]	0.075	0.005

All data are expressed as median (25; 75 percentile). GY4137 was administered 12 and 18 hours after induction of fecal peritonitis, i.e., after the 12 hour time point. Control: n=8, GY4137 n=8 (n=9 for troponin). #: p<0.05 vs 12 hours of peritonitis (before administration of GY4137) within group.

Table 5: Parameters of renal function and injury.

	Before peritonitis	12h peritonitis	24h peritonitis	Repeated measures two-way ANOVA	
				p value for treatment	p value for time
Urine output (mL*kg⁻¹*h⁻¹)	Vehicle GY4137 8.0 (6.3; 10.6) 3.7 (2.5; 6.0)	5.1 (2.3; 6.6) 3.3 (1.6; 4.4)	1.4 (0.6; 3.5) [#] 0.8 (0.3; 1.7)	0.268	0.007
Renal artery flow (ml*min⁻¹)	Vehicle GY4137 112 (60; 267) 175 (107; 200)	68 (45; 190) 180 (83; 194)	45 (0; 117) [#] 100 (29; 161) [#]	0.312	<0.001
Renal venous pO₂ (mmHg)	Vehicle GY4137 46 (43; 55) 45 (39; 51)	48 (42; 51) 49 (44; 57)	48 (38; 53) 45 (37; 55)	1.0	0.017
Renal venous pH	Vehicle GY4137 7.51 (7.49; 7.55) 7.52 (7.45; 7.53)	7.49 (7.48; 7.50) 7.46 (7.46; 7.52)	7.45 (7.34; 7.51) [#] 7.42 (7.36; 7.47) [#]	0.739	<0.001
Renal venous base excess (mmol¹*L⁻¹)	Vehicle GY4137 6.9 (6.3; 7.7) 7.5 (4.0; 8.1)	6.6 (5.4; 7.5) 5.2 (3.4; 6.4)	6.6 (5.4; 7.5) 2.7 (-0.3; 4.4) ^{#,§}	0.020	<0.001
Renal venous lactate (mmol¹*L⁻¹)	Vehicle GY4137 2.3 (1.8; 2.8) 2.7 (1.8; 3.2)	2.3 (1.6; 2.5) 2.6 (1.9; 2.9)	4.6 (2.3; 6.1) [#] 3.1 (2.6; 6.0) [#]	0.961	<0.001
Arterial creatinine (µmol¹*L⁻¹)	Vehicle GY4137 114 (101; 126) 102 (95; 115)	108 (101; 128) 106 (101; 121)	135 (116; 192) [#] 130 (115; 159) [#]	0.456	<0.001
Creatinine clearance (mL*min⁻¹)	Vehicle GY4137 67 (53; 85) 62 (57; 72)	69 (38; 78) 73 (61; 78)	47 (26; 65) 47 (33; 78)	0.562	0.042
Blood NGAL (ng*L⁻¹)	Vehicle GY4137 66 (52; 94) 77 (66; 83)	236 (169; 261) 199 (182; 226)	485 (388; 610) [#] 365 (323; 584) [#]	0.270	<0.001

All data are expressed as median (25; 75 percentile). GYY4137 was administered 12 and 18 hours after induction of fecal peritonitis, i.e., after the 12 hour time point. Control: n=8, GYY4137 n=9 animals. #: p<0.05 vs 12 hours of peritonitis (before administration of GYY4137) within group. §: p<0.05 vs vehicle.

Supplemental table 1: Mitochondrial respiration

		heart	kidney	liver
OxPhos ($\mu\text{mol}\cdot\text{mg}^{-1}\cdot\text{s}^{-1}$)	Vehicle	283 (261; 338)	111 (93; 131)	52 (52; 65)
	GY4137	306 (263; 390)	128 (115; 138)	59 (52; 54)
ETS ($\mu\text{mol}\cdot\text{mg}^{-1}\cdot\text{s}^{-1}$)	Vehicle	310 (278; 393)	126 (117; 139)	90 (77; 95)
	GY4137	385 (325; 413)	146 (131; 152)	100 (84; 120)
LEAK/ETS (%)	Vehicle	30 (21; 40)	29 (24; 49)	53 (41; 77)
	GY4137	34 (21; 38)	26 (18; 38)	60 (41; 80)

All data are expressed as median (25; 75 percentile). vehicle: n=5, GY4137 n=5 (n=4 for liver). OxPhos: maximal oxygen flux related to oxidative phosphorylation (in the coupled state), ETS: maximal respiratory capacity of the electron transfer system in the uncoupled state, LEAK/ETS: respiration compensation for proton leakage or slipping, expressed as percentage of ETS.